Supplement

Table S1. Models from the Coupled Model Intercomparison Project Phase 5 (CMIP5) used for this study.

Model Name	Institute
ACCESS1-0	Commonwealth Scientific and Industrial Research,Organization (CSIRO) and Bureau of Meteorology (BOM), Australia
BCC-CSM1-1	Beijing Climate Center, China Meteorological Administration
BNU-ESM	College of Global Change and Earth System Science, Beijing Normal University
CanESM2	Canadian Centre for Climate Modelling and Analysis
CNRM-CM5	Centre National de Recherches Météorologiques / Centre Européen de Recherche et Formation Avancée en Calcul Scientifique
CSIRO-Mk3.6.0	Commonwealth Scientific and Industrial Research Organization in collaboration with Queensland Climate Change Centre of Excellence
HadGEM2-CC	Met Office Hadley Centre (additional HadGEM2-ES realizations contributed by Instituto Nacional de Pesquisas Espaciais)
HadGEM2-ES	Met Office Hadley Centre (additional HadGEM2-ES realizations contributed by Instituto Nacional de Pesquisas Espaciais)
INM-CM4	Institute for Numerical Mathematics
IPSL-CM5A-LR	Institut Pierre-Simon Laplace
IPSL-CM5A-MR	Institut Pierre-Simon Laplace
IPSL-CM5B-LR	Institut Pierre-Simon Laplace
MIROC-ESM	Japan Agency for Marine-Earth Science and Technology, Atmosphere and Ocean Research Institute (The University of Tokyo), and National Institute for Environmental Studies
MIROC-ESM-CHEM	Japan Agency for Marine-Earth Science and Technology, Atmosphere and Ocean Research Institute (The University of Tokyo), and National Institute for Environmental Studies
MIROC5	Atmosphere and Ocean Research Institute (The University of Tokyo), National Institute for Environmental Studies, and Japan Agency for Marine-Earth Science and Technology
MRI-CGCM3	Meteorological Research Institute
NorESM1-M	Norwegian Climate Centre

Table S2. Models from the Atmospheric Chemistry and Climate Model Intercomparison Project (ACCMIP) used for this study (Lamarque et al, 2013).

Model	Type	Resolution(lat/lon/#levels), top level	Modelling Center
NCAR-CAM3.5	CCM	1.875/2.5/L26, 3.5 hPa	NCAR,USA
GFDL-AM3	CCM	2/2.5/L48, 0.017 hPa	UCAR/NOAA,GFDL, USA
MIROC-CHEM	CCM	2.8/2.8/L80, 0.003 hPa	FRCGC, JMSTC Japan
GISS-ModelE2*	CCM	2/2.5/L40, 0.14 hPa	NASA-GISS,USA

*We use an updated GISS simulation relative to their ACCMIP contributions, forced in atmospher-only mode using the ACCMIP emissions (Lamarque et al., 2010), observed daily sea-surface temperatures and sea-ice from Reynolds et al. (2007), and with winds nudged to the Modern-Era Retrospective Analysis for Research and Applications (MERRA) meteorological reanalysis (Rienecker et al., 2011).

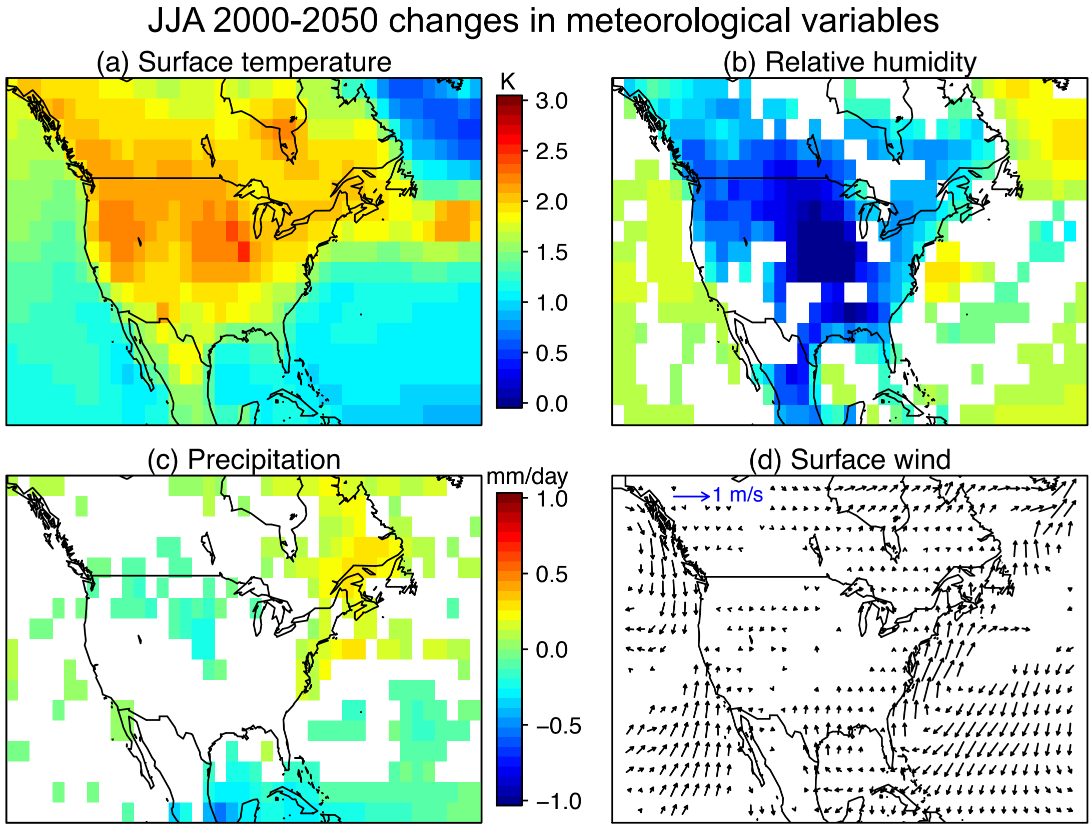

Figure S1. Seasonal changes in June-July-August (a) mean temperature, (b) relative humidity, (c) precipitation and (d) surface wind field from 2000-2019 to 2050-2069, as projected by 17 CMIP5 climate models following the RCP4.5 scenario. White space indicates regions where fewer than 70% of the models show a consistent sign of change.

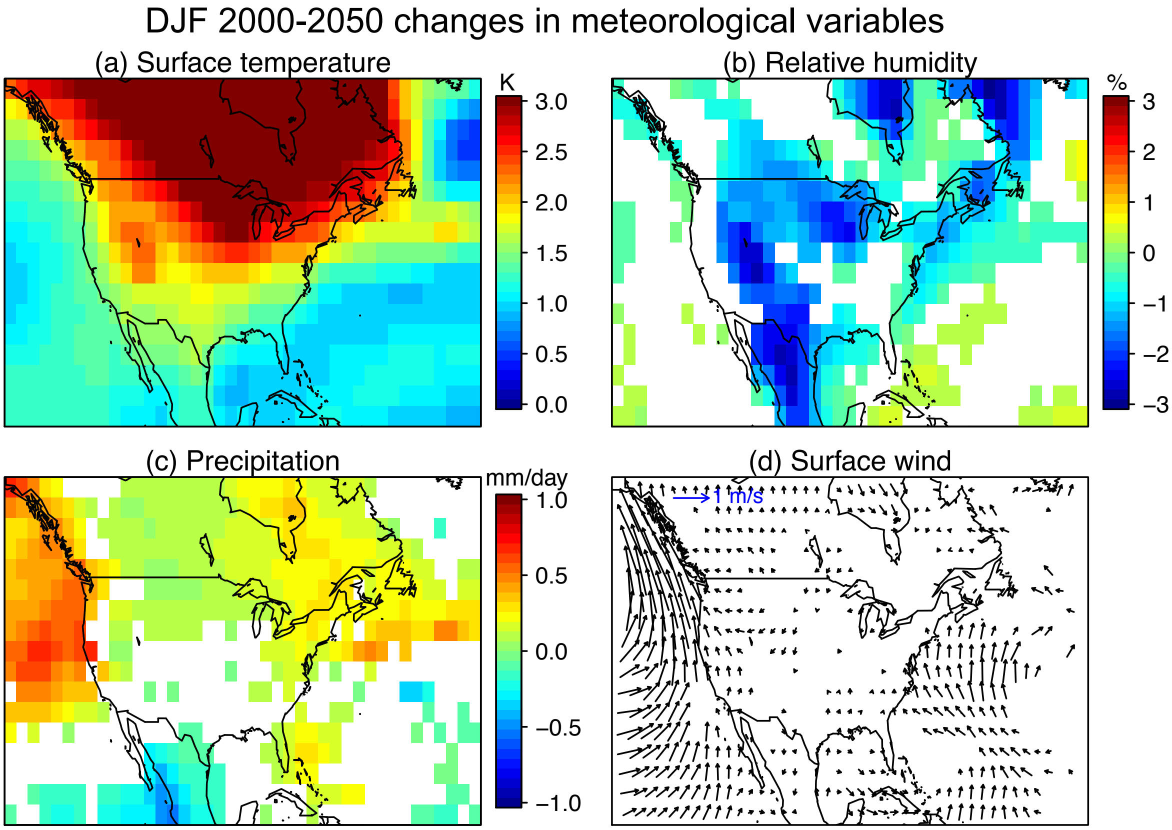

Figure S2. Same as Figure S1 but for December-January-February.

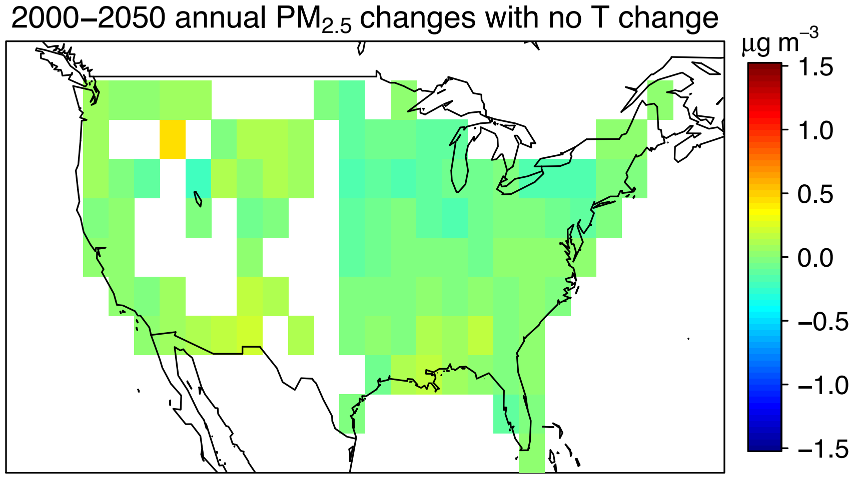

Figure S3. Response of annual mean $PM_{2.5}$ concentrations to 2000-2050 climate change when changes in surface temperature are excluded. The figure shows the mean response as projected by an ensemble of 17 CMIP5 models. For this sensitivity test, surface temperatures in the statistical model for 2050-2069 are kept the same as for 2000-2019. White areas indicate regions with no $PM_{2.5}$ observations.

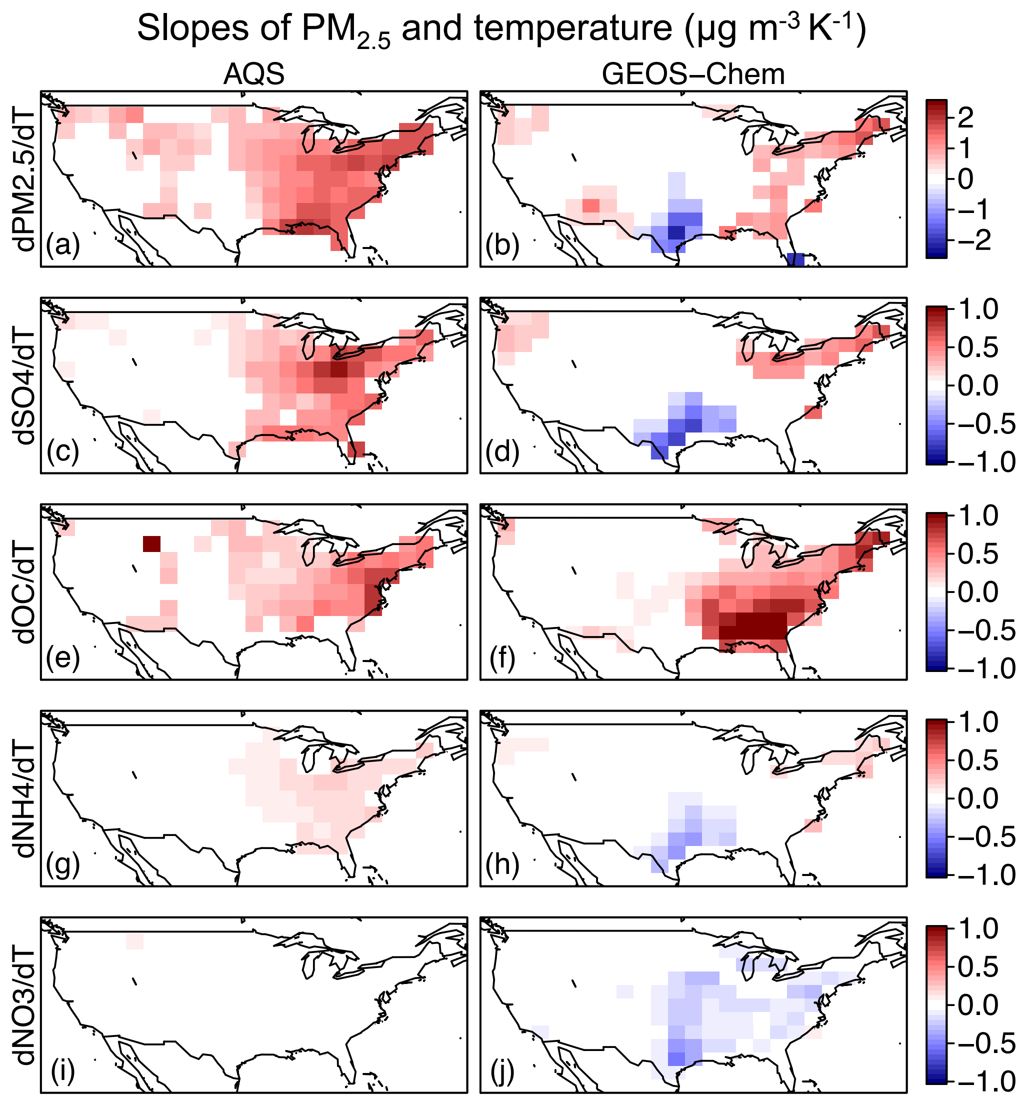

Figure S4. The slopes of detrended (a-b) monthly mean $PM_{2.5}$ and (c-j) different $PM_{2.5}$ components with surface air temperature for 2004-2012 summer months. Left column shows slopes from AQS observations, and right column shows results from GEOS-Chem. Panels a and b are the same as Figures 6a and 6f. White areas indicate either missing data or grid boxes where the slope is not significant at the 0.05 level.

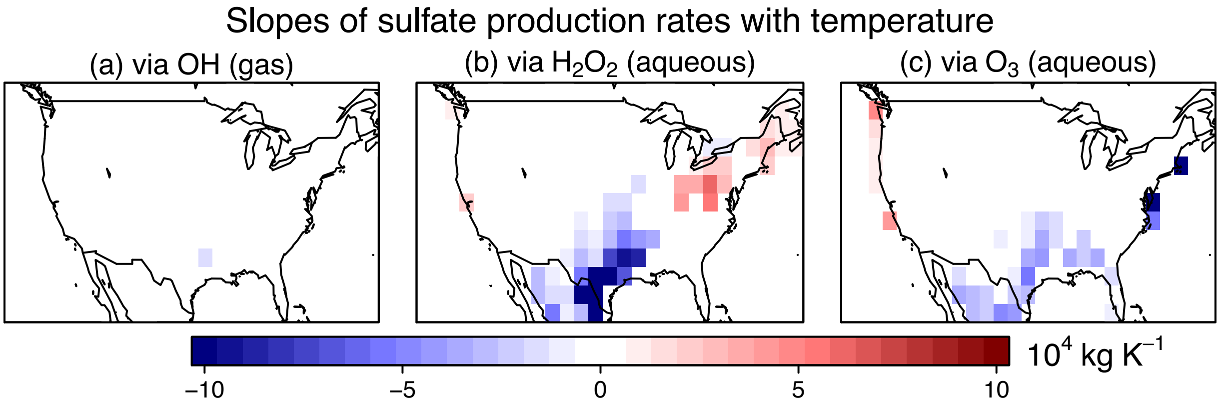

Figure S5. Slopes of monthly mean sulfate production with surface air temperature for 2004-2012 summer months, as calculated by GEOS-Chem. The panels show slopes from three different production pathways: (a) gas-phase oxidation by OH and aqueous-phase oxidation by (b) H_2O_2 and (c) O_3. See Section 5 for more details. White areas indicate either missing data or grid boxes where the slope is not significant at the 0.05 level.